Pramāṇa – J. Phys., Vol. 29, No. 3, September 1987, pp. 261–277. © Printed in India.

Laser photoacoustic spectroscopy of iodine molecule: Single and two-photon absorption

PUTCHA VENKATESWARLU,* G CHAKRAPANI,†
M C GEORGE, Y V RAO†† and C OKAFOR

Department of Physics, Alabama A&M University, Normal (Huntsville), AL 35762, USA
†On leave from the Indian Institute of Technology, Kanpur, India
††On leave from A.N.R. College, Gudivada, India

MS received 2 January 1987

Abstract. Photoacoustic spectroscopy of iodine molecule has been studied in gas phase using nitrogen laser-pumped tunable dye laser. The experiment yielded the vibrational spectrum corresponding to $X^1\Sigma^+(0_g^+) \rightarrow B^3\Pi(0_g^+)$ transition up to the convergence limit. The photoacoustic spectrum in the region 17580–18850 cm^{-1} is presented along with the vibrational analysis. Five of the vibrational bands reported earlier by Venkateswarlu, Kumar and McGlynn have been partially resolved and the structure of one of them has been analyzed and shown to be due to an overlap of (14, 2) and (12, 1) bands. The analysis was based on a comparison with the highly resolved spectrum of Gerstenkorn and Luc. The structure observed in the region 20200–20750 cm^{-1} which is beyond the convergence limit of the transition $X^1\Sigma^+(0_g^+) \rightarrow B^3\Pi(0_u^+)$ has been analyzed as due to two-photon absorption. Most of the bands could be assigned to two transitions both originating in the ground state and terminating in two different electronic states 1_g and $E(0_g^+)$, at $T_e = 40821$ cm^{-1} (or $T_0 = 41355$ cm^{-1}) and $T_e = 41411$ cm^{-1} (or $T_0 = 41355$ cm^{-1}) respectively.

Keywords. Photoacoustic spectroscopy; iodine; single-photon absorption; two-photon absorption.

PACS Nos 33·10; 33·20

1. Introduction

Photoacoustic spectroscopy is a good technique to study non-radiative relaxations in atomic, molecular and solid state systems (Rosencwaig 1980; Pao 1977; Kumar *et al* 1983). Dissociations and predissociations, vibrational and rotational relaxations and energy transfers between neighbouring states in molecules can be conveniently studied by this technique (Patel and Tam 1981; Tennel *et al* 1985; Reddy *et al* 1981; Rottenberg *et al* 1983). Halogens and mixed halogens are good candidates for such studies using this technique (Venkateswarlu *et al* 1984) for various reasons. In I_2, Br_2 and Cl_2 different repulsive curves are expected to touch or cross the $B^3\Pi(0_u^+)$ state (Mulliken 1934, 1971; Asundi and Venkateswarlu 1947). Fluorescence experiments of Kruzel *et al* (1971) indicated the existence of vibrational and rotational relaxations in the B state of I_2 and it is expected that similar relaxations occur in the other halogens. The spin orbit interaction splittings ($^2P_{3/2}$ $^2P_{1/2}$) in F, Cl, Br and I are 404·0, 882·36, 3685·15 and 7605·15 cm^{-1} respectively (Moore 1971, Venkateswarlu *et al* 1984).

If one obtains the halogen atoms in $^2P_{1/2}$ state by photodissociation of a suitable molecule containing a halogen atom, energy is released when the atom undergoes

transition from $^2P_{1/2}$ to $^2P_{3/2}$ state. Laser action in atomic iodine and bromine is based on this principle. Photoacoustic spectroscopy may be used conveniently to determine the vertical energies required to dissociate the molecule to give $^2P_{1/2}$ halogen atomic species. Iodine atomic laser action has been achieved by using solar radiation to produce I ($^2P_{1/2}$) atoms by photodissociating C_2F_5I (DeYoung and Weaver 1986), C_3F_7I (Lee and Weaver 1981) and n-C_4F_9I (DeYoung 1986) molecules.

Venkateswarlu *et al* (1984) studied the photoacoustic spectra of I_2 and ICl in the regions 15150–17520 cm^{-1} and 16040–17280 cm^{-1} respectively. They also recorded the I_2 spectrum in the region 18900–20000 cm^{-1}. Their analyses show that the spectrum of I_2 is due to the transition $X^1\Sigma_g^+ \rightarrow B^3\Pi(0_u^+)$ while that of ICl is due to the transition $X^1\Sigma^+ \rightarrow A^3\Pi(1)$. The excitation source used by them was a Chromatax CMX-4 flash lamp pumped tunable dye laser of peak power 8 kW and pulse width ~ 1 μsec (Kumar *et al* 1983).

In the present study the photoacoustic spectrum of I_2 has been recorded in the region 15900–20750 cm^{-1} using a sensitive photoacoustic spectrometer built in the laboratory and a dye laser pumped by a 900 kW N_2 laser. The vibrational analysis has been extended to include the bands in the region 17580–18850 cm^{-1}. Some of the bands in the region 16500–17000 cm^{-1} have been partially resolved and the results of the analysis of one of them together with those of the extended vibrational analysis are presented in this paper. The analysis of the photoacoustic spectrum in the region 20200–20750 cm^{-1} which lies beyond the convergence limit of the $X \rightarrow B$ transition reveals two-photon absorptive transitions from the ground state to two different upper electronic states lying in the region 40700–41750 cm^{-1}. The results obtained are also described in this paper.

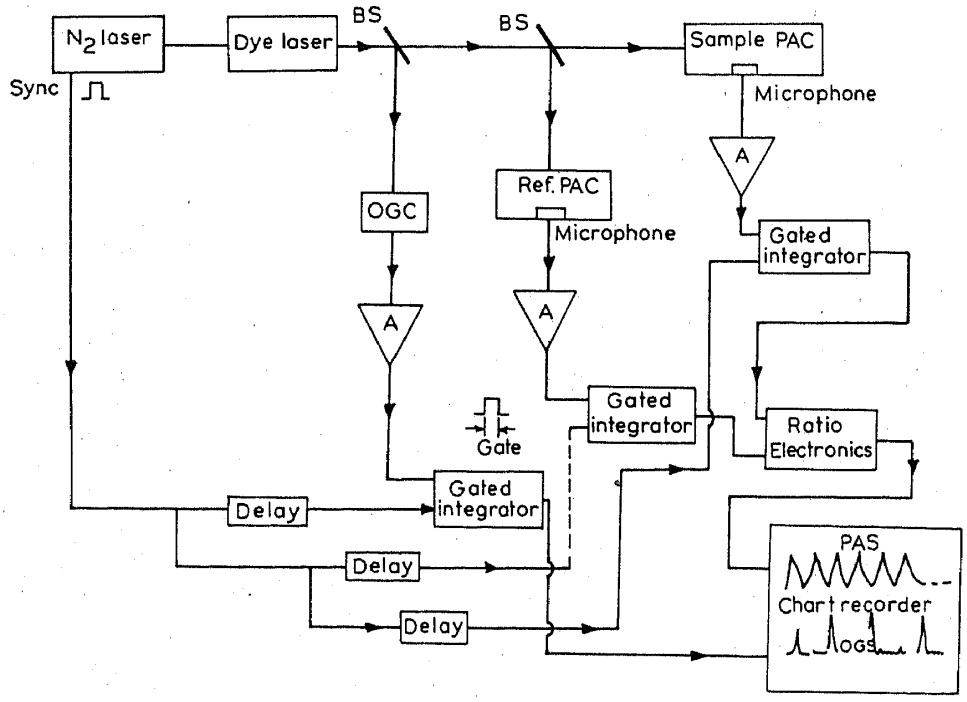

Figure 1. Block diagram of the experimental arrangement for photoacoustic spectroscopy.

2. Experimental procedure

The photoacoustic spectrometer used for studies in gas phase is described elsewhere (Chakrapani *et al* 1987) and only a brief description will be presented here. Figure 1 shows the block diagram of the experimental set-up used in the present work. The excitation source used in these experiments is a tunable dye laser (Molectron model DLII) pumped by a nitrogen laser (Model UV24) with a variable pulse repetition rate of 1–50 pps. Typical output from the dye laser is 200 μJ per pulse. In normal operation the bandwidth of the dye laser output is approximately 0·3 cm^{-1} which can be further reduced to about 0·03 cm^{-1} using an intracavity etalon.

The dye laser beam is steered to enter the system through a variable aperture so as to remove fluorescent background. About 10% of this beam is focussed into a uranium-neon hollow cathode lamp (Buck Scientific Inc) to excite the optogalvanic spectrum. The remaining 90% of the dye laser beam enters the aluminum box through an optical (quartz) window fitted to one side of the box. The laser beam after entering the box is again split into two parts of unequal intensity, one of 90% and the other of 10%. The weaker beam is focussed onto a reference photoacoustic cell filled with burnt wood shavings which acts as a broad-band energy detector. The absorbed laser energy is detected as an acoustic signal by an electret microphone (Knowles Electronics, model BT-1759) placed inside the cell. This signal is amplified by a preamplifier of switchable gain of 1000 or 5000 and of bandwidth of approximately 20 kHz.

The stronger of the two beams enters the photoacoustic cell containing iodine at a saturated vapour pressure of 0·4 torr in the presence of atmospheric air. The laser beam excites some of the molecules in the cell from the ground to the excited state. The excited molecules transfer part of their excited energy through non-radiative relaxation processes to the gas in the cell which results in a slight increase in its temperature and hence its pressure. The pressure pulse thus generated propagates and causes acoustic ringing which is detected by another microphone placed at the end of a side tube attached to the photoacoustic cell at its middle. The output signal of the microphone is amplified by a preamplifier similar to the one used to amplify the reference signal. The photoacoustic and the reference cells as well as the preamplifiers are assembled in the rigid air-tight aluminium box to minimize the environmental acoustic noise and the electromagnetic interference from the pulsed nitrogen laser. The amplified signal from the photoacoustic cell, after being averaged by a gated integrator which is also triggered by the nitrogen laser after a delay of 500 μsec, is normalized with respect to a similarly processed signal from the reference cell. The normalized signal which takes into account any fluctuations in the intensity of the laser beam is recorded on a strip chart recorder. The optogalvanic spectrum of Ne which serves as a calibration spectrum is recorded simultaneously with the photoacoustic spectrum of I_2.

3. Analysis and results

3.1 *Photoacoustic spectrum due to the absorptive transition* $X^1\Sigma^+(0_g^+) \rightarrow B^3\Pi(0_u^+)$

The photoacoustic spectrum of I_2 has been recorded in the region 15900–2075 cm^{-1}. A portion of the spectrum obtained in the regions 17580–18850 cm^{-1} is reproduced in

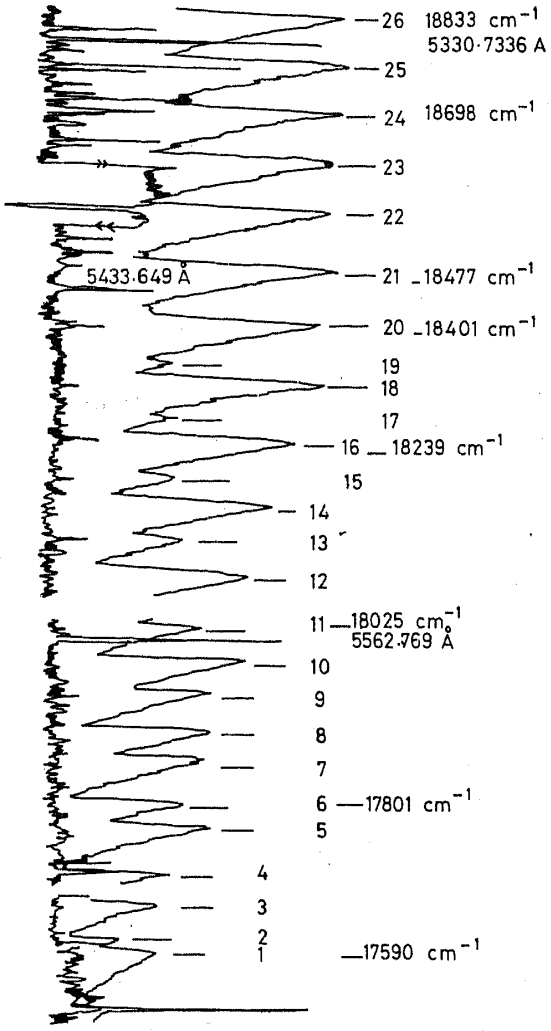

Figure 2. Photoacoustic spectrum of I_2 in the region 18840–17600 cm^{-1}.

figure 2 in which the bandheads are numbered serially. The figure also shows the optogalvanic spectrum of neon recorded simultaneously for calibration purposes. The wavelengths of the bandheads were calculated by fitting a number of neon standard lines to a quadratic or cubic equation by least squares method and converted to vacuum wavenumbers using Edlin's (1953) formula. The wavenumbers of the band heads measured in the region are given in table 1. The accuracy of measurements is estimated to be ± 1 cm^{-1} for bands with sharp heads and about ± 2 cm^{-1} for others. All the bands could be analyzed as belonging to two different v' progressions of the $X^1\Sigma^+(0_g^+) \rightarrow B^3\Pi(0_u^+)$ systems of I_2. The vibrational assignments and the wavenumbers of the band heads calculated using the known constants of the two states (Luc 1980) are also presented in the table for the purpose of comparison. The calculated and observed wavenumbers agree within the accuracy of measurement of the latter. This clearly shows that the photoacoustic spectrum arises chiefly as a result of non-radiative relaxation processes through which the photo-excited molecules in the $B^3\Pi(0_u^+)$ state transfer a part of their excitation energy and the deexcited molecules in the ground state a part of their rovibrational energy to the medium in the cell. Additional contribution

Table 1. Band head positions (cm^{-1}) in the photoacoustic spectrum of I_2 and vibrational assignments.

Sl. No.	Present exp.	Calculated (Luc's data)	Vibrational assignment	Sl. No.	Present exp.	Calculated (Luc's data)	Vibrational assignment
1	17590	17588	19-1	14	18154	18155	23-0
2	17614	17613	17-0	15	18187	18187	26-1
3	17680	17680	20-1	16	18239	18239	24-0
4	17708	17708	18-0	17	18264	18264	27-1
5	17769	17769	21-1	18	18320	18321	25-0
6	17801	17801	19-0	19	18340	18340	28-1
7	17858	17857	22-1	20	18401	18400	26-0
8	17894	17893	20-0	21	18477	18478	27-0
9	17941	17942	23-1	22	18553	18553	28-0
10	17983	17982	21-0	23	18626	18626	29-0
11	18025	18026	24-1	24	18698	18698	30-0
12	18069	18070	22-0	25	18766	18767	31-0; 38-2
13	18109	18105	25-1	26	18833	18834	32-0

to the photoacoustic signal may come from predissociation of the molecules in the excited state, if any.

3.2 *Partially resolved rotational structure of the (14, 2), (12, 1) bands in the photoacoustic spectrum*

Five bands in the region 16500–17000 cm^{-1} with their heads at 16573, 16681, 16787, 16891 and 16991 cm^{-1} have been partially resolved. The spectrum showing the partially resolved rotational structure of one of them in the region 16797–16895 cm^{-1} is shown in figure 3. There are 73 rotational features in this region all of which are numbered serially in the figure. To analyze this structure it was necessary to first identify the rotational lines in the corresponding region of the atlas of the absorption spectrum of I_2 recorded by Gerstenkorn and Luc (1978). For this purpose the wavenumbers of the rotational lines due to different rotational-vibrational transitions expected in this region were calculated using the molecular constants of Luc (1980). The rotational lines in the atlas were identified by comparing their measured wavenumbers with the calculated ones. The fact that the rotational structure of the $X \rightarrow B$ transitions of I_2 consists of PR doublets and the $P(J)$ and $R(J)$ lines corresponding to odd J values are expected to be stronger than those corresponding to even J values because of different statistical weights (Venkateswarlu 1977) greatly facilitated the identification. On the basis of this identification most of the relatively strong lines in the region 16797–16895 cm^{-1} of the atlas are found to be the rotational lines belonging to 14, 2 and 12, 1 bands which overlap each other in this region.

A comparison of the photoacoustic spectrum with the rotational structure of the absorption bands in the I_2 atlas, thus identified, reveals that each rotational feature in the spectrum represents the envelope of two or more close-lying doublets belonging to the two overlapping bands. The wavenumbers of the rotational features together with the analysis in terms of their corresponding $P(J)$, $R(J)$ designations are given in table 2.

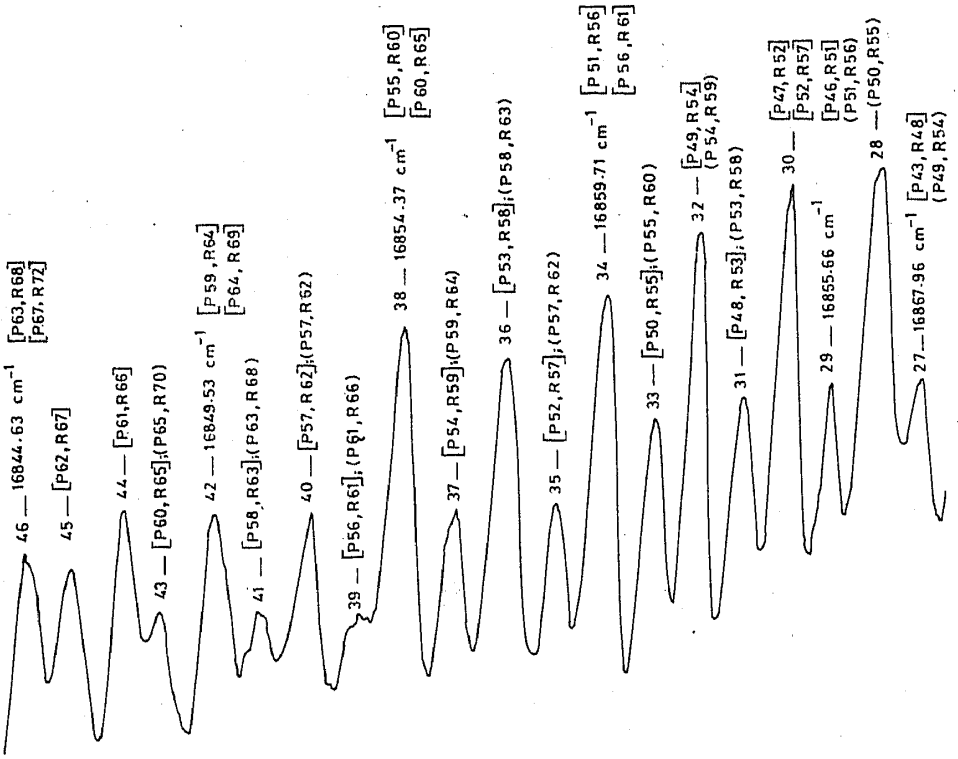

Figure 3b. Partial rotational structure of the (14, 2) and (12, 1) bands of I_2 showing alteration of intensities in the region 16868–16844 cm^{-1}.

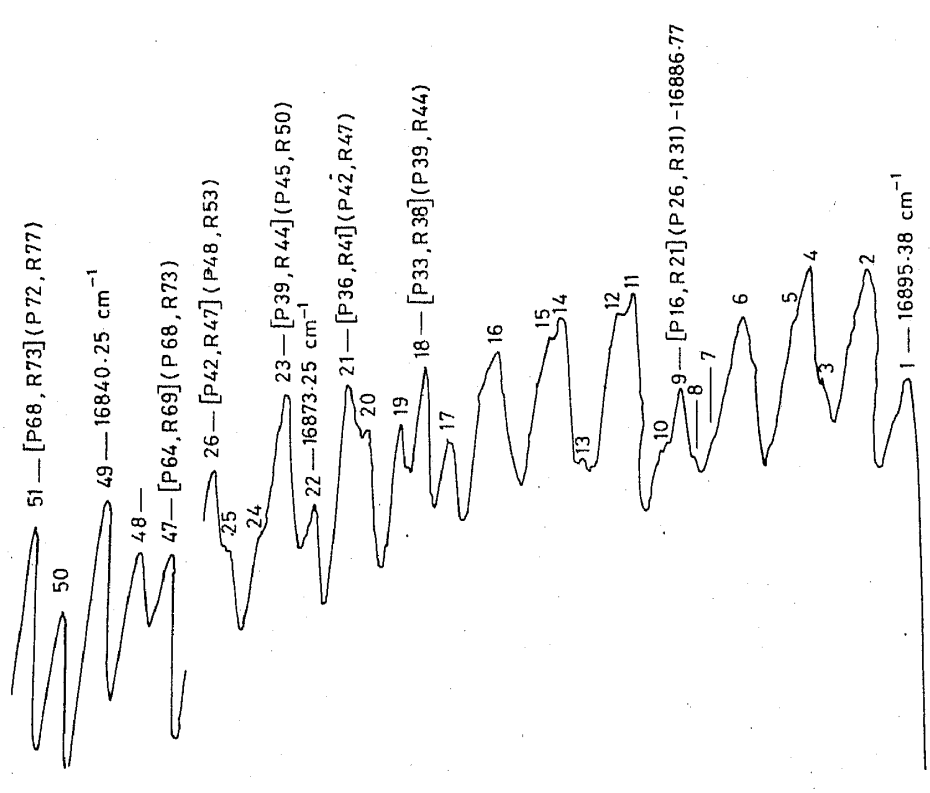

Figure 3a. Partial rotational structure of the (14, 2) and (12, 1) bands of I_2.

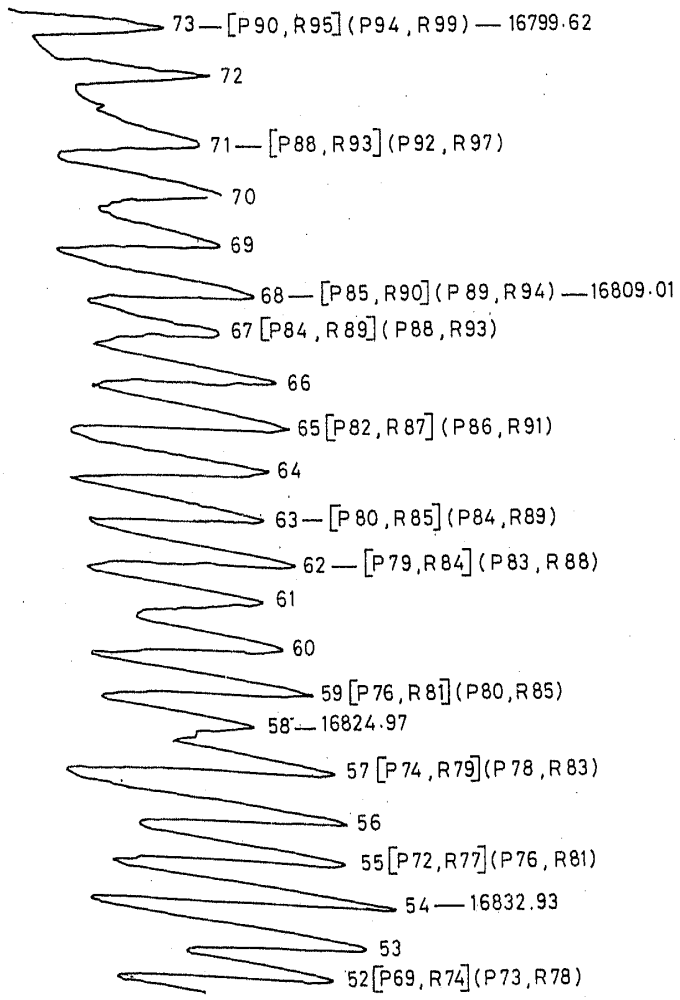

Figure 3c. Partial rotational structure of the (14, 2) and (12, 1) bands in the region 16384–16794 cm^{-1}.

An interesting aspect of the partially resolved rotational spectrum is that the intensity of the rotational features varies alternately in the region 16844–16868 cm^{-1}. The portion of the spectrum showing the intensity alternation is enlarged and reproduced in figure 3b. Each rotational feature in this region corresponds to an envelope of two absorption doublets belonging to (14, 2) and (12, 1) absorption bands. From the individual intensities of the $P(J)$ and $R(J)$ lines in the two doublets in the atlas corresponding to any rotational feature, it is possible to estimate the intensity of the absorption envelope that might conceivably exist in the place of the unresolved doublet. Such estimated intensities are also found to vary alternately in this region but in a manner opposite to that observed in the photoacoustic spectrum thereby implying that a strong absorption in this region gives rise to a weak photoacoustic signal and vice versa contrary to the general expectation. Although the reason for the alternation of the intensities of the rotational features is not clear, a plausible explanation for this might, however, be sought in terms of possible near coincidences between some of the rovibrational levels in the upper or lower state of these bands and those in the same or possibly neighbouring electronic states. If such coincidences occur for alternate rotational levels associated with the upper or lower vibrational levels of the 14-2 or 12-1

Table 2. Partially resolved rotational structure in the (14, 2) and (12, 1) bands of I_2 in the photoacoustic spectrum and its correlation with the resolved structure in I_2 atlas (a).

Sl. No.	ν (cm^{-1}) observed	Relative intensity	Remark (b)	Band (c) (14, 2)		Band (c) (12, 1)	
				$P(J)$	$R(J)$	$P(J)$	$R(J)$
1	16895·38	15	M			1–7	6–12
2	16893·71	31	S			8–13	13–18
3	16892·31	3	h			—	—
4	16891·68	37	S			16–17	21–22
5	16891·08	5	h	—	—	—	—
6	16889·25	31	S	4–10	9–15	21–22	26–27
7	16888·03	7	h	—	—	—	—
8	16887·43	8	h	—	—	—	—
9	16886·77	21	M	16	21	26	31
10	16886·10	12	h	—	—	—	—
11	16884·77	40	S	20–21	25–26	29–30	34–35
12	16884·31	31	h	22	27	31	36
13	16883·09		W	—	—	—	—
14	16882·10	39	S	25	30	33	38
15	16881·74	36	h	—	—	—	—
16	16879·76	36	S	28–30	33–35	36–37	41–42
17	16878.08	23	M	—	—	—	—
18	16877·16	37	S	33	38	39	44
19	16876·40	28	M	34	39	40	45
20	16875·18	29	h	35	40	41	46
21	16874·40	39	S	36	41	42	47
22	16873·25	20	M	37–38	42	43–44	48–49
23	16872·13	42	S	39	44	45	50
24	16871·22	10	h	40	45	46	51
25	16870·10	19	h	41	46	47	52
26	16869·45	34	S	42	47	48	53
27	16867·96	20	M	43	48	49	54
28	16866·93	49	S	45	50	50	55
29	16865·66	46	M	46	51	51	56
30	16864·52	52	S	47	52	52	57
31	16863·38	28	M	48	53	53	58
32	16862·08	52	S	49	54	54	59
33	16861·05	31	M	50	55	55	60
34	16859·71	48	S	51	56	56	61
35	16858·48	23	M	52	57	57	62
36	16857·19	44	S	53	58	58	63
37	16855·80	26	M	54	59	59	64
38	16854.37	50	S	55	60	60	65
39	16853·34	15	W	56	61	61	66
40	16852·05	30	M	57	62	62	67

Table 2 (*Contd.*)

Sl. No.	ν (cm^{-1}) observed	Relative intensity	Remark (b)	Band (c) (14, 2)		Band (c) (12, 1)	
				$P(J)$	$R(J)$	$P(J)$	$R(J)$
41	16850·76	19	W	58	63	63	68
42	16849·53	34	S	59	64	64	69
43	16848·19	23	M	60	65	65	70
44	16847·13	38	S	61	66	—	—
45	16845·63	33	M	62	67	—	—
46	16843·06	38	M	63	68	67	72
47	16843·06	36	M	64	69	68	73
48	16841·78	38	M	65	70	69	74
49	16840·25	50	S	66	71	70	75
50	16838·75	32	M	67	72	71	76
51	16837·42	50	S	68	73	72	77
52	16836·02	43	M	69	74	73	78
53	16834·52	51	S	70	75	74	79
54	16832.93	58	S	71	76	75	80
55	16831·35	50	S	72	77	76	81
56	16829·86	53	S	73	78	77	82
57	16828·09	51	S	74	79	78	83
58	16826·55	36	M	75	80	79	84
59	16824·97	47	S	76	81	80	85
60	16823·40	41	S	77	82	81	86
61	16821·70	37	S	78	83	82	87
62	16820·16	43	S	79	84	83	88
63	16818·48	37	S	80	85	84	89
64	16816·49	38	S	81	86	85	90
65	16814·41	42	S	82	87	86	91
66	16812·63	40	S	83	88	87	92
67	16810·92	36	S	84	89	88	93
68	16809·01	31	S	85	90	89	94
69	16807·13	30	S	86	91	90	95
70	16805·22	35	S	87	92	91	96
71	16803·34	29	S	88	93	92	97
72	16801·40	24	S	89	94	93	98
73	16799·62	36	S	90	95	94	99

(a) Gerstenkorn and Luc (1978)
(b) The letters W, M and S in column 4 stand for weak, medium and strong intensities, and h stands for hump.
(c) The numbers in the last four columns represent J values.

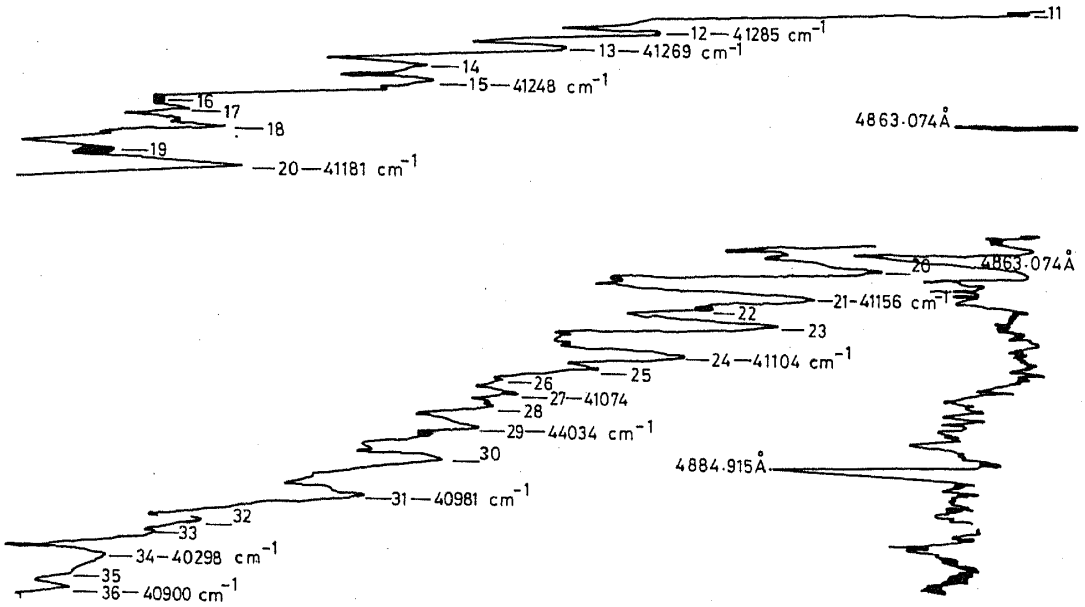

Figure 4a. Two-photon photoacoustic spectrum of I_2 in the region 41300–40900 cm^{-1}.

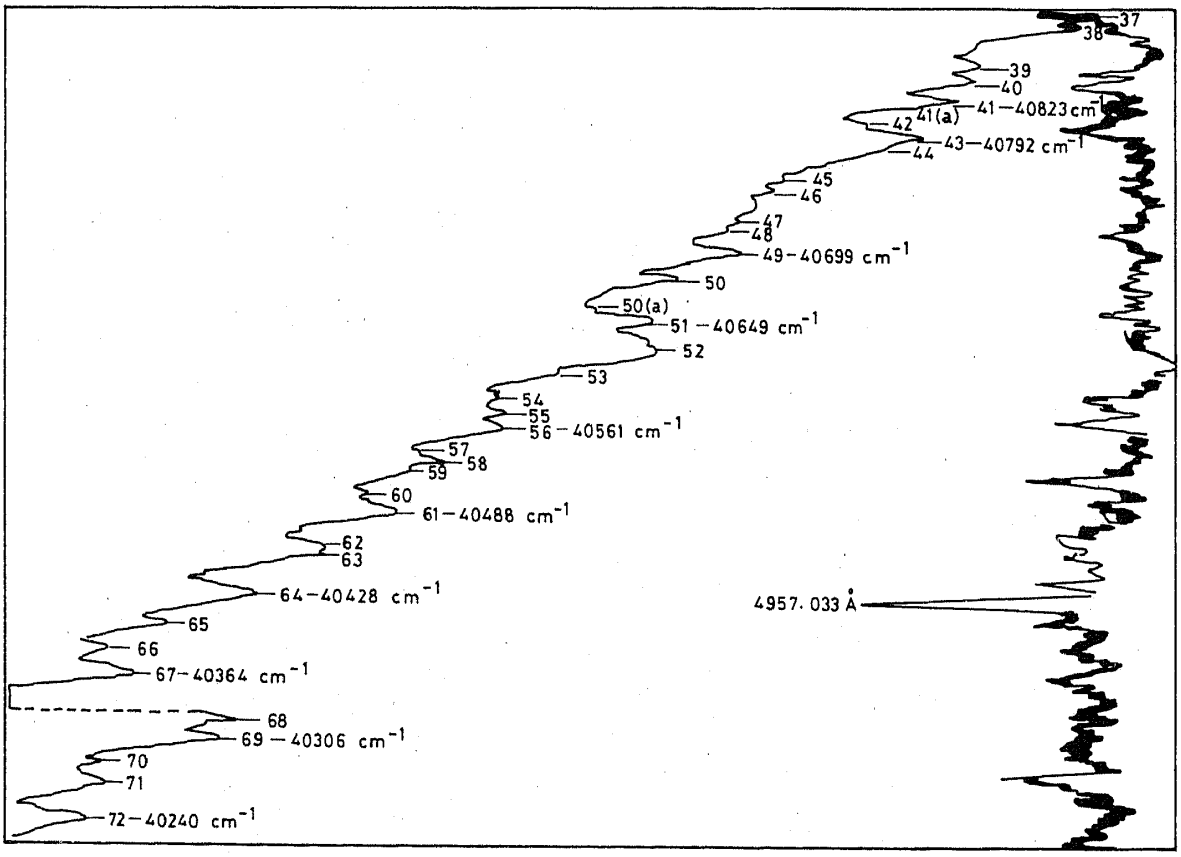

Figure 4b. Two-photon photoacoustic spectrum of I_2 in the region 40900–40240 cm^{-1}.

band, one expects an enhancement in the intensity of the photoacoustic rotational features that involve transitions from or to these levels. This is so because near coincidences ($\Delta E < kT$) between energy levels of any pair of molecules enhance the cross-section for resonant energy transfer from one to the other, the excess or deficit in energy (ΔE) appearing as a change in the energy of the medium in the cell which in turn appears as a photoacoustic signal. The opposite nature of the variation in intensity of the absorption and photoacoustic features in this region, perhaps, indicates that the resonance energy transfer from the alternate rotational levels is so effective as to modify the latter beyond normal expectation.

Another noteworthy aspect of the spectrum is the sudden increase in its intensity in the region above 16844 cm^{-1}. This probably indicates the crossing of the $B^3\Pi(0_u^+)$ state by a repulsive curve at about $v'=14$, $J'=54$ or $v'=12$, $J'=59$ rovibrational level; as such a crossing results in the dissociation of the molecules in the levels at and above the crossing point with consequent enhancement in the corresponding photoacoustic signal.

3.3 *Two-photon photoacoustic spectrum*

The photoacoustic spectrum of I_2 is weak beyond the convergence limit of the $X \rightarrow B$ system but shows a slowly rising hump with a distinct structure in the region 20200–20750 cm^{-1}. To increase the intensity, this region of the photoacoustic spectrum was recorded by focussing the laser beam in the photoacoustic cell using a short focus lens and the spectrum obtained is shown in figures 4(a) and (b) in which the discrete structure comes out to be intense and clear. As there are no stable states of I_2 in the region between the dissociation limit of the $B^3\Pi(0_u^+)$ state at 20052 cm^{-1} and the limit corresponding to the dissociation products $I(^2P_{1/2})+I(^2P_{1/2})$ at 27657 cm^{-1}, no single photon absorptive transition from the ground state can be expected to account for the observed structure. The only possible way in which this structure could be understood appears to be through multi-photon absorption process very possibly a two-photon process.

Attempts were made to analyze the spectrum as due to two-photon transitions from the ground state to one or more upper electronic states lying at about 41000 cm^{-1} above the ground state. Venkateswarlu *et al* (1986) discussed the electronic states arising out of different configurations in the region 40000–47060 cm^{-1}. They suggested that the 1_g state (β state of King *et al* 1981) at $T_0=40766$ cm^{-1} observed by Perrot *et al* (1983) could be the $^3\Sigma^-(1_g)$ arising from the configuration $\sigma_g^2\pi_u^2\pi_g^4\sigma_u^2$ while the 0_g^+ component of $^3\Sigma_g^-$ state could be identified with the $E(0_g^+)$ at $T_0=41355$ cm^{-1} observed by them and other groups (Wieland *et al* 1972; Brand *et al* 1982; Brand and Hoy 1983). From the known vibrational constants of these two states and those of the ground state (Luc 1980), the Deslandres schemes for the two transitions $E(0_g^+)\leftarrow X$ and $\beta(1_g)\leftarrow X$ were developed.

The positions of the band maxima in the region 20200–20750 cm^{-1} using the optogalvanic spectral lines of the Ne for calibration are given in table 3 with a multiplication factor of 2. They represent an average of four sets of values obtained from four different recordings of the spectrum. The estimated error in the measurement is ± 2 cm^{-1} for sharp maxima and ± 3 cm^{-1} for others. By comparing the calculated wavenumbers of the bands in the Deslandres schemes with twice the measured wavenumbers of the bands in the spectrum, it was found that all but a couple of the

Table 3. Observed photoacoustic spectral data and their vibrational assignments to two-photon transition in I_2.

		$\beta(1_g) \leftarrow X^1\Sigma^+(0_g^+)$			$E(0_g^+) \leftarrow X^1\Sigma^+(0_g^+)$		
Sl. No.	Observed exp. values (cm^{-1}) × 2	Calculated values (cm^{-1})	Vibrational assignment v^1, v''	O–C	Calculated values (cm^{-1})	Vibrational assignment v^1, v''	O–C
1	41492	41489	7,0	3			
2	41462				41456	1,0	6
3	41447				41444	3,1	3
4	41401				41403	9,4	−2
5	41384	41387	6,0	−3			
5a	41369	41366	10,2	3			
6	41352				41355	0,0	−3
7	41342				41344	2,1	−2
8	41329				41331	4,2	−2
9	41316				41319	6,3	−3
10	41308				41305	8,4	3
11	41296				41292	10,5	4
12	41285	41285	5,0	0			
13	41269	41266	9,2	3			
14	41256						
15	41248				41243	1,1	5
16	41233				41232	3,2	1
17	41221				41220	5,3	1
18	41211				41207	7,4	4
19	41197				41196	9,5	1
20	41181	41182	4,0	−1			
21	41556	41555	10,3	1			
22	41146				41142	0,1	4
23	41134				41131	2,2	3
24	41104				41108	6,4	−4
25	41092				41098	8,5	−6
26	41083	41079	3,0	4	41086	10,6	−3
27	41074	41072	5,1	2			
28	41061	41064	7,2	−3			
		41055	9,3	6			
29	41032				41031	1,2	3
30	41015				41021	3,3	−6
					41010	5,4	5
31	40981	40975	2,0	6			
32	40958	40962	6,2	−4			
33	40948	40954	8,3	−6			
		40945	10,4	4			
34	40928				40930	0,2	−2
35	40909				40911	4,4	−2
36	40900				40901	6,5	−1
37	40886				40891	8,6	−5
					40880	10,7	6
38	40866	40866	3,1	0			
		40871	1,0	−5			

Table 3. (*Contd*).

		$\beta(1_g) \leftarrow X^1\Sigma^+(0_g^+)$			$E(0_g^+) \leftarrow X^1\Sigma^+(0_g^+)$		
Sl. No.	Observed exp. values (cm^{-1}) × 2	Calculated values (cm^{-1})	Vibrational assignment v^1, v''	O–C	Calculated values (cm^{-1})	Vibrational assignment v^1, v''	O–C
39	40852	40853	7,3	−1			
40	40841	40846	9,4	−5			
41	40823				40820	1,3	3
41(a)	40815				40811	3,4	4
42	40802				40802	5,5	0
43	40792				40793	7,6	−1
44	40767	40766	0,0	1			
45	40759	40762	2,1	−3			
		40757	4,2	2			
46	40747	40751	6,3	−4			
		40745	8,4	2			
47	40722				40719	0,3	3
48	40710				40711	2,4	−1
49	40699				40694	6,6	5
50	40676				40676	10,8	0
50a	40659	40658	1,1	1			
51	40649	40653	3,2	−4			
		40649	5,3	0			
52	40632	40637	9,5	−5			
53	40606				40611	1,4	−5
					40603	3,5	3
54	40592				40595	5,6	−3
					40587	7,7	5
55	40575				40578	9,8	−3
56	40561						
57	40549	40550	2,2	−1			
		40546	4,3	3			
58	40531	40536	8,5	−5			
		40530	10,6	1			
59	40524	40530	10,6	6			
60	40508				40510	0,4	2
					40503	2,5	5
61	40488				40488	6,7	0
62	40465						
63	40452	40446	1,2	6			
64	40428	40430	9,6	2			
65	40403				40402	1,5	1
66	40383				40389	5,7	6
					40382	7,8	1
67	40364						
68	40325	40329	8,6	−4			
69	40306				40301	0,5	5
70	40294				40296	2,6	−2
					40290	4,7	−4
71	40268						
72	40240	40235	1,3	5			

Table 4. Expected band head positions (cm^{-1}) for the two-photon transition $\sigma_g^2\pi_4^2\pi_g^4\sigma_4^{23}\Sigma_g^-(1_g)-\sigma_g^2\pi_4^4\pi_g^{41}\Sigma^+(0_g^+)$ in I_2 (Bands identified with those in the present two-photon photoacoustic absorption are underlined.)

v' \ v''	0	1	2	3	4	5	6
0	40766	40553	40341	40130	39920	39712	39505
	(+1)						
1	40870	40658	40446	40235	40025	39817	39610
	(−5)	(+1)	(+6)	(+5)			
2	40975	40762	40550	40339	40129	39921	39714
	(+6)	(−3)	(−1)				
3	41079	40866	40653	40443	40233	40024	39818
	(+4)	(0)	(−4)				
4	41182	40969	40757	40546	40336	40127	39921
	(−1)		(+2)	(+3)			
5	41285	41072	40859	40649	40439	40231	40024
	(0)	(+2)	(+1)	(0)			
6	41387	41174	40962	40751	40541	40333	40126
	(−3)		(−4)	(−4)			
7	41489	41276	41064	40853	40643	40435	40228
	(+3)		(−3)	(−1)	(+6)		(−3)
8	41591	41377	41165	40954	40745	40536	40329
				(−6)	(+2)	(−5)	(−4)
9	41692	41478	41266	41055	40845	40631	40430
			(+3)	(+6)	(−5)	(−5)	(+2)
10	41792	41578	41366	41155	40945	40737	40530
			(+3)	(+1)	(+4)		(+1)

Values in paranthesis give the differences between two times the observed values and the calculated values.

observed bands could be attributed to the two transitions $E(0_g^+)\leftarrow X$ and $\beta(1_g)\leftarrow X$. The calculated Deslandres schemes of these two transitions are given in tables 4 and 5. Those calculated values which agree with twice the wavenumbers of the observed band heads are underlined in the Deslandres schemes. The number in parenthesis given under each such band indicates the difference between the observed and the calculated values (O–C). The vibrational assignments of the bands along with the (O–C) deviations are included in table 3.

3.4 *Discussion*

As indicated earlier the photoacoustic spectrum, in all probability is due to the rotational vibrational relaxations in the upper and lower electronic states involved in the transitions. Such relaxations in the upper state of the $X-B$ transitions of I_2 have been demonstrated unambiguously by the fluorescence work of Kruzel *et al* (1971). Additionally, there could be similar relaxations between the rovibrational levels of one electronic state and those of the neighbouring electronic states as demonstrated by the work of Koffend *et al* (1983) (see below).

Table 5. Expected band head positions (cm^{-1}) for the two-photon transition $E(0_g^+)$—$X^1\Sigma^+(O_g^+)$ in I_2 (bands identified with those in the present two-photon photoacoustic absorption are underlined.)

v' v''	0	1	2	3	4	5	6	7	8
0	41355	41142	40930	40719	40510	40301	40094	39888	39684
	(−3)	(+4)	(−2)	(+3)	(+2)	(+5)			
1	41456	41243	41031	40820	40611	40402	40195	39989	39785
	(+5)	(+5)	(+3)	(+3)	(−5)	(−1)	(+4)		
2	41557	41344	41131	40920	40711	40503	40296	40090	39885
		(−2)	(+2)		(−1)	(+5)	(−2)		
3	41657	41444	41232	41021	40811	40603	40396	40190	39985
		(+3)	(+1)	(−6)	(+4)	(+3)			
4	41757	41543	41331	41121	40911	40703	40496	40290	40085
			(−2)		(−2)	(+7)	(−4)	(−4)	
5	41856	41643	41431	41220	41010	40802	40595	40389	40185
				(+1)	(+5)	(0)	(−3)	(+6)	
6	41955	41742	41530	41319	41108	40901	40694	40488	40283
				(−3)	(−4)	(−1)	(+5)	(0)	
7	42054	41841	41628	41418	41207	41000	40793	40587	40382
					(+4)		(−1)	(+5)	(+1)
8	42152	41939	41727	41516	41305	41098	40891	40685	40480
					(+3)	(−6)	(−5)		
9	42250	42036	41824	41614	41403	41196	40989	40783	40578
					(−2)	(1)			(−3)
10	42347	42035	41922	41711	41500	41292	41086	40880	40676
						(+4)	(−3)	(+6)	(0)

Values in parenthesis give the differences between two times the observed values and calculated values.

One sees from table 3 that the two-photon photoacoustic spectrum involved transitions from the higher vibrational levels up to $v''=8$. Similar involvement of higher vibrational levels up to $v''=5$ in the single photon photoacoustic spectrum has been reported earlier by Venkateswarlu *et al* (1984). The involvement of such high vibrational levels at room temperature, though a little unexpected, is not inexplicable. In general when molecules are excited to an upper electronic state, radiative transitions to different vibrational levels right up to the dissociation limit of the ground state take place (Verma 1960). As I_2 is a homopolar molecule, the only way a molecule in any one of the higher vibrational levels can lose its energy is through collisional non-radiative relaxation processes. This restriction on the relaxation pathways possibly explains the non-equilibrium distribution of molecules in the higher vibrational levels of the ground state and hence their involvement in the photoacoustic spectrum. I_2 molecules when excited to the $E(0_g^+)$ or $\beta(1_g)$ states appear to be trapped in those states as direct radiative transitions from these states to the ground state $^1\Sigma^+(0_g^+)$ are parity-forbidden and hence not allowed. However, it is possible for the molecules to go from the *gerade* states like $E(0_g^+)$ and $\beta(1_g)$ states to the neighbouring *ungerade* states like $D(0_u^+)$ and

gerade states like $D'(2_g)$ respectively through collisions. The molecules in the $D(0_u^+)$ states can undergo radiative transitions to different vibrational levels of the ground state while those in the $D'(2_g)$ state can first come down to $A'(2_u)$ state giving fluorescence and then to different vibrational levels of the ground state through collisions. The reality of these different possibilities has been established by Koffend *et al* (1983) by their observation $D'(2_g) \rightarrow A'(2_u)$ and $D(0_u^+ \rightarrow X^1\Sigma^+(0_g^+)$ transitions in induced fluorescence.

One expects a considerable increase in the photoacoustic intensity in the region of dissociation of the molecule. Such a significant increase is not noticed in the present experiments indicating that the dissociation product $^2P_{1/2}$ atom does not contribute much to the photoacoustic intensity by losing its energy through non-radiative relaxations. However, it might be contributing partly to the general background of the photoacoustic spectrum in the concerned region.

Plans are underway to extend the present investigations to higher frequency region to look for the photoacoustic spectrum involving two-photon absorption from the ground state of I_2 to the following gerade electronic states: (i) $\gamma(0_g^+)$ with $T_e = 41621\ \text{cm}^{-1}$ (King *et al* 1981), (ii) $f(0_g^+)$ with $T_e = 47026\ \text{cm}^{-1}$ (Brand and Hoy 1983) and (iii) 1_g, with $T_e = 47559\ \text{cm}^{-1}$ (Viswanathan *et al* 1981). The range of photon frequencies needed for this work (20800–24000 cm^{-1}) will be conveniently available from the tunable dye laser in the visible region. Experiments are also to be planned to carry out the experiments at different laser powers to find out the nature of the dependence of the photoacoustic spectral intensity I_p on the input laser intensity I_1. As $I_p \propto I_1^n$, where n represents the number in the n photon absorption process, these experiments will enable the determination of the value of n. In the contemplated experiments n is expected to come out as 2.

4. Acknowledgements

This work was supported by the US Department of Energy Grant No. DE-F05-84-ER13206. We would like to thank Professor S P Mc Glynn, Dr D Kumar and Dr H Jagannath for their kind help in getting this work started.

References

Asundi R K and Venkateswarlu P 1947 *Indian J. Phys.* **21** 101
Brand J C D and Hoy A R 1983 *J. Mol. Spectrosc.* **97** 389
Brand J C D, Hoy A R, Kalkar A K and Yamashita 1982 *J. Mol Spectrosc.* **95** 350
Chakrapani G, Venkateswarlu P, Rao Y V and George M C 1987 *Rev Sci. Instrum.* (in press)
DeYoung R J 1986 *IEEE J. Quantum Electron.* **QE-22** 1019
DeYoung R J and Weaver W R 1986 *Appl. Phys. Lett.* **49** 369
Edlen B 1953 *J. Opt. Soc. Am.* **43** 339
Gerstenkorn S and Luc P 1978 *Atlas der Spectre. d' Absorption de la Molecule de L' iode* (14800–20000 cm^{-1}), Editions du G N R S Paris, France
King G W, Littlewood I H and Robins J R 1981 *Chem. Phys. Lett.* **56** 145
Koffend J B, Sibai A M and Bacis R 1983 Collisionally induced optical-optical double resonance in I_2: Rotational Analysis of the D' (2g)- A' (2u) Laser Transition (Private Communication)
Kumar D, Nauman R V, Mohanty R, McGlynn P and Findley G L 1983 *Rev. Sci. Instrum.* **54** 463
Kruzel R B, Steinfeld J I, Holtzenbuhler D A and Leroi G E 1971 *J. Chem. Phys.* **55** 4822
Lee Ja H and Weaver W R 1981 *Appl. Phys. Lett.* **39** 137
Luc P 1980 *J. Mol. Spectrosc.* **80** 41

Moore C E 1971 *Atomic energy levels* (Washington D.C: National Bureau of Standards) Vols 1–3
Mulliken R S 1934 *Phys. Rev.* **46** 549
Mulliken R S 1971 *Chem. Phys.* **55** 288
Pao Y H (ed.) 1977 *Optoacoustic spectroscopy and detection* (New York: Academic Press)
Patel L K N and Tam A C 1981 *Rev. Mod. Phys.* **53** 517
Perrot J P, Broyer M, Chevaleyre J and Femelat B 1983 *J. Mol. Spectrosc.* **98** 161
Rosencwaig A (ed.) 1980 *Photoacoustics and photoacoustic spectroscopy* (New York: John Wiley)
Reddy K V and Berry M J 1981 Photoacoustic spectroscopy, MB4 Technical Digest Second Int. Topical Meeting Optical Society of America, New York
Rottenberg L J, Bernstein B and Peters K S 1983 *J. Chem. Phys.* **79** 2569
Tennel K, Rose A, Pyrum J, Muzny C, Gupta R and Salamo G 1985 in *Lasers as reactants and probes in chemistry* (eds) W M Jackson and A B Harvey (Washington DC: Howard University Press) p. 431
Venkateswarlu P 1977 *Indian J. Phys. Commem. Vol* **II** 273
Venkateswarlu P, Kumar D and McGlynn S P 1984 *Proc. Symp. on Lasers and Applications* (eds) H D Bist and J S Goela (New Delhi: Tata McGraw-Hill)
Venkateswarlu P, Pramela T and Rao Y V 1986 *Spectrochim. Acta* **A42** 285
Verma R D 1960 *J. Chem. Phys.* **32** 738
Viswanathan K S., Sur A and Tellinghuisen 1981 *J. Mol. Spectrosc.* **86** 393
Wieland K, Tellinghuisen J B and Nobbs A 1972 *J. Mol. Spectrosc.* **41** 69